Arc Phenomena and Gasdynamic Effects due to Interaction of Shock Waves with Magnetic Fields

H. KLINGENBERG

Institut für Plasmyphysik, 8046 Garching/München, Germany

(Z. Naturforsch. **23 a**, 1929—1939 [1968]; received 18 September 1968)

The arc phenomena occurring on interaction of shock-heated plasma with a magnetic field were studied in order to achieve an approximately uniform current distribution in a certain volume using a number of small electrodes. This is necessary for producing plane gasdynamical effects such as reflected shocks and one-dimensional flow behind them in order to compare experimental results with theory. The current amplitude depends on the surface area and the number of electrodes. It is governed by the complex boundary conditions in the plasma-to-electrode transition, which consists of narrow current channels leading to arc spots. Streak photographs show that the flow is slowed down, and reflected fronts are observed which can be interpreted as shock fronts taking relaxation effects into account.

Since many plasma experiments involve complicated interactions between shock waves and magnetic fields, it is interesting to study such phenomena under simple conditions. A suitable example is provided by plane shock waves with a perpendicular magnetic field. At high shock Mach numbers, a plasma streaming with supersonic velocity $\boldsymbol{v}$ (with respect to the local velocity of sound) is produced behind the front. If the streaming plasma is now acted on by a transverse magnetic field $\boldsymbol{B}$, the charge carriers are subjected to $\boldsymbol{v} \times \boldsymbol{B}$ forces. Currents of density $\boldsymbol{j}$ can then flow through electrodes flush mounted on the inside of the shock tube and connected on the outside. The plasma is therefore subjected to retarding $\boldsymbol{j} \times \boldsymbol{B}$ forces directed opposite to the velocity $\boldsymbol{v}$ and is slowed down. Strong reduction of the plasma velocity results in secondary gasdynamic effects, such as reflected shock waves. Theoretical treatment even of one-dimensional flow entails considerable mathematical difficulties since the interaction process is described by a system of coupled, non-linear partial differential equations. Theoretical studies have therefore been restricted so far to one-dimensional flow with transverse magnetic field and uniform current perpendicular to the field and the flow. Plane secondary fronts are thus obtained as solutions. The most comprehensive theoretical investigations of this kind were conducted by REBHAN[1]. This author studied the final, asymptotic, steady state of ideal gases outside the interaction region. Recently, JOHNSON[2] investigated the steady and unsteady states of an ideal gas in the interaction region. Both of these authors find that when the interaction is sufficiently strong there should be a reflected plane shock wave and rarefaction waves, the latter modifying the intensity of the primary shock front.

Experiments allowing comparison with theoretical results thus have to satisfy (approximately at least) such simple conditions as one-dimensional flow, transverse magnetic field, and uniform, transverse current, the latter condition being difficult to meet.

All known experimental investigations have been conducted on shock tubes with electrodes of large surface area flush mounted along the inside of the tube and connected on the outside. All authors assume that the current comes from the entire electrode surface and uniformly fills the interaction region. In these experiments reflected luminous fronts have also been observed by means of streak pictures. Many investigations of this type have been conducted by, for example, PAIN and co-workers[3].

The results of the first interaction experiments conducted in our laboratory[4] on a diaphragm shock tube fitted with single pairs of electrodes of large surface area showed, however, that the current flows in the form of arcs which may strike the electrodes at different points from one shot to the next. A number of arc spots can already be observed on the electrodes after one shot. The current density distribution is then governed by the

[1] E. REBHAN, Report IPP 3/28, August [1965].
[2] M. R. JOHNSON, Phys. Fluids **10**, 539 [1967].
[3] H. J. PAIN, and P. R. SMY, Brit. J. Appl. Phys. **7**, 1585 [1966].
[4] H. KLINGENBERG, and H. MUNTENBRUCH, Report IPP 3/45, November [1966].

complicated boundary conditions prevailing in the narrow current channels in front of the electrode spots. It is certainly not *uniform*. The assumption of uniform current density distribution that has been made by various authors is therefore questionable. Comparison of their results with the theory is of doubtful validity.

The purpose of the investigations described here is to achieve experimentally a uniform current distribution (approximately at least) in order to fulfill the conditions of the theory.

Using heated electrodes capable of providing the required high current densities of several hundred amperes per square centimetre would entail very difficult technological problems. The arc phenomenon was therefore utilized by mounting many electrodes of small surface area alongside and behind one another and short-circuiting the pairs separately in an attempt to produce many arcs alongside and behind one another in order to achieve a good approximation of the required uniform current distribution in the interaction volume.

Interaction effects were also investigated.

I. Experimental Set-Up

The shock tube (inner diameter 10 cm, length approx. 13 m) is of the diaphragm type. The driving gas is hydrogen (100 atm) and the test gas is argon (e.g. 1 torr). For $p_0 = 1$ torr the shock Mach number at the measuring site (9 m from the diaphragm region) is then $M_s = 11.8$, the equilibrium temperature behind the shock front 10^4 °K, the flow velocity of the plasma 3 mm/μsec and the conductivity 40 mhos, cf. [4].

The measuring chamber has a square internal cross section [(7×7) cm^2]. A well-known method using a sharp cutter is used to cut out the rectangular flow from the circular flow of the shock tube. The measuring chamber is made of plexiglass and, owing to the danger of breakage, it is constructed in sections, these being sealed with 0-rings and secured between tie plates. The total length of the chamber with cutters is about 1 m.

Various sizes and numbers of electrodes were used. A few measurements were made with one electrode pair having a surface area of (3×7) cm^2 (3 cm in the flow direction). These electrodes projected slightly from the wall, and so they were tapered in both directions. Most of the measurements, however, were made with small electrodes 4.5 mm in diameter, first with one pair, then with five pairs transverse to the flow direction and five pairs in the flow direction, and finally with 25 pairs. The centre-to-centre distance between the pairs is 1.4 cm.

Each electrode pair was short-circuited separately with a copper bridge. When several electrode pairs were used the bridges were of various lengths. The total external DC resistance (bridges + electrodes) therefore varied between 1.1 and 1.6 mΩ. It was determined by a current-voltage measuring method, cf. [4]. The corresponding AC resistance was calculated, and it varied between 2.7 and 4 mΩ. The total inductance of each discharge circuit was measured with an inductance meter. For this purpose, the bridge was short-circuited between the electrodes with a wire, cf. [4]. The inductance varied between 0.3 and 0.55 μHy. The values 3 mΩ and 0.4 μHy can be taken as the mean values for resistance and inductance respectively. This value of the external resistance was small compared to the internal resistance.

The magnetic field was produced with a crowbarred capacitor bank (10 kV, 30 kJ) via coils similar to the Helmholtz type. The magnetic field strength was 6.8 kG and fairly constant during the interaction period. In the interaction region the magnetic field was still uniform to a certain extent.

The currents from the plasma were measured with Rogowski coils mounted on top of the short-circuiting bridges. The signals of the coils were electronically integrated and then recorded by an oscilloscope, with the display calibrated directly in units of current. Owing to the limited number of integration units present not more than five coils were used at any one time, these being shifted in succession (with more than five electrode pairs present). Two types of coils were used, viz. a large coil (type I) for measurements involving only one electrode pair and five small coils (type II) for the other measurements. The coils of the latter type are so alike that they agree in sensitivity to within 3%. After electronic integration the sensitivity is:

Type I: 158 mV/kA

Type II: 46 mV/kA.

The vBd voltage (v = flow velocity, B = magnetic field strength, d = interelectrode distance) produced between two electrodes was measured with a potentiometer circuit. One pair of electrodes was bridged with a 100 kΩ resistance series connected with a 50 Ω resistance. The voltage, which drops at the 50 Ω resistance, was fed by a 50 Ω cable direct to the input of an ungrounded oscilloscope. The circuit was calibrated with a square-wave signal of known voltage.

For triggering, measuring the shock front velocity, and recording the luminous effect in the plasma, photomultipliers were used. The spatial resolution was improved by installing the multipliers behind slit systems. Observations were made on a level with the longitudinal axis of the measuring chamber.

The luminous effect was recorded by means of image converters. For this purpose there were two three-picture cameras mounted at right angles to one another to convey a three-dimensional impression. The effects due to interaction were recorded with a drum camera. For the streak pictures a 5 mm wide slit running the entire length of the measuring chamber was stopped down and imaged on the film.

II. Results

1. Oscillograms and image converter pictures

Fig. 1a—c shows some oscillograms and image converter pictures for various electrode configurations. The most important features are explained below:

For large electrodes the current starts immediately on arrival of the shock front at the electrodes (comparison between multiplier and current signals). The shape of the current signal, see dJ/dt signal, is very continuous as opposed to that in the case of small electrodes, see below. The image converter pictures, particularly those taken from above, show how arcs strike at several points indicated by a higher degree of incandescence. These pictures clearly suggest a *non-uniform* current distribution. The side-on pictures show at first more incandescence near the electrodes, i.e. where the arcs strike. It is only later that the gas becomes more incandescent over the entire cross section of the measuring chamber.

For one pair of small electrodes the current starts in the relaxation region and the current amplitude is lower. The image converter pictures also show the shock front (only in the first set of measurements using a new plexiglass section in the measuring chamber) and the plasma boundary, defining in this way the relaxation region. The side-on photograph clearly shows the strong incandescence near the electrodes, i.e. where the arcs strike in the relaxation region. The picture taken from above also shows this incandescence. On passing through the narrow current channels leading to the electrodes the gas is excited to strong incandescence. After the gas has passed through them, this incandescence takes some time to disappear.

For five electrode pairs transverse to the flow direction the current flows through all five pairs, has nearly the same time behaviour and can generally be reproduced well (superimposed is the noise signal from the crowbar discharge). It starts in the relaxation region. The time at which the individual arcs start are different. Some do not start until the current maximum of the others is reached. This delay in starting can also be observed in the image converter pictures taken from below. In side-on observation, the gas becomes incandescent over the entire cross section of the measuring chamber, there being a slight bulge in the flow direction.

For 25 electrode pairs the current amplitude is lower than with 5 pairs. (The oscillogram is taken from a set where the bridges of the individual rows alternately face in the opposite directions. The superimposed noise signals from the crowbar discharge are then much smaller, and the current signal is recognized more readily. The Rogowski coils in this example are mounted on the bridges of the 3rd row of electrodes). The time behaviour is again very similar. (Sometimes the starting time of the individual arcs is different, as in the case of 5 electrode pairs.) The image converter picture taken from below shows again the striking of the arcs and the delay in striking. It can thus be checked whether current has flowed through all 25 electrode pairs. The side-on picture shows strong incandescence over the entire cross section, there being again a slight bulge in the flow direction. These pictures suggest a rather uniform current density distribution in the interaction volume.

The $v \cdot B \cdot d$ signal is superposed on the dJ/dt signal from the crowbar discharge. In the shock front it makes an upward jump and is of approximately rectangular form.

The multiplier signals in front of the interaction region (Fig. 1a, b*) display the usual behaviour, viz. a small peak in the shock front, a rise in the relaxation region, a decrease after equilibrium (caused by radiation cooling), and a decline in the contact front. The peak in the shock front still appears behind the interaction region and allows the velocity of the primary shock front after interaction to be measured (first multiplier oscillogram in Fig. 1c).

Especially at higher pressures there appear in the relaxation region secondary peaks, from which it can be concluded that there are many secondary fronts present. Behind the interaction region these fronts are more pronounced (second multiplier oscillogram in Fig. 1c).

2. Results of vBd measurements

Fig. 2 shows the calculated and measured values of the vBd voltage. (v can be calculated with allowance for ionization since the shock Mach number is known.) The error spread of the calcu-

* Figs. 1, 6, 7, 8 see Table 1932 a—d and Table 1932 e, f.

lated values is governed essentially by the accuracy of the measured shock front velocity, cf. [4]. Only for $p_0 = 1$ torr do the error spreads of the measured and calculated values fail to overlap. The mean deviation (dashed curve) is only 15%. This indicates that no strong eddy currents are present in the plasma.

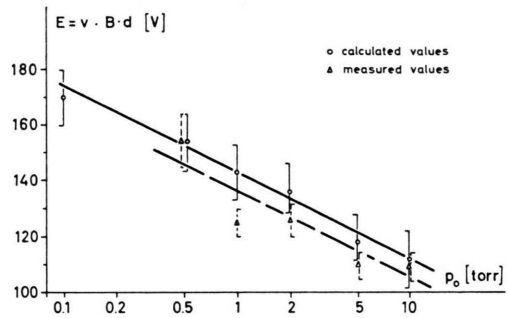

Fig. 2. Calculated and measured values of vBd voltage. $B = 6.8$ kG, $d = 7$ cm. One pair of small electrodes.

3. *Results of current measurements*

Particularly with 25 electrode pairs the current was more irregular. Therefore the integral mean values with respect to time:

$$\overline{J} = \frac{1}{t_2 - t_1} \cdot \int_{t_1}^{t_2} J(t) \cdot \mathrm{d}t ,$$

t_1 = time at which the arc strikes (just behind the shock front),

t_2 = time of disruption (in the contact front),

$t_2 - t_1$ = pulse length of current.

seemed to be a better criterion for calculating the retarding $j \times B$ force than the maximum current. These values were therefore formed from all oscillograms of the current by using a planimeter. Here the spurious signal from the crowbar discharge, which is recorded separately for each set of measurements, was substracted from the total signal. This integral mean value is 25% lower on the average than the maximum value.

Table 1 shows in kA the arithmetic mean values of these evaluations of many current measurements, i.e. of the integral mean values, for various electrode configurations. These configurations are denoted by symbols, which are also shown in Table 1 A.

The mean value of the integral mean current per electrode pair of small surface area decreases with the number of electrodes. This is almost irrespective of whether the electrode pair (in the case of one pair) is located in the centre or at the boundary of the chamber or whether the electrode pairs (in the case of five pairs, for example) are transverse or parallel to the flow direction.

The direction of the bridges here does not have any noticeable influence on the current value, nor does the distance between the short-circuited electrode pairs. This decrease with the number of electrodes is illustrated in Fig. 3.

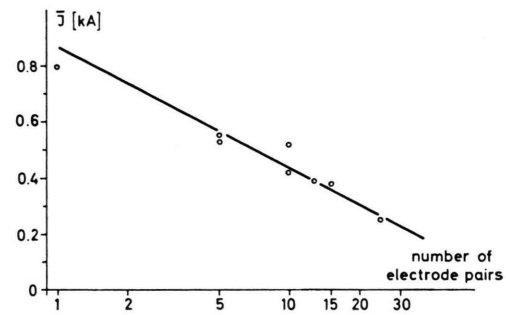

Fig. 3. Current per electrode pair vs. number of electrode pairs.

The current flowing through the large electrode is much higher. This variation of the current amplitude with the surface area of the electrodes has been observed before [4]. This dependence is shown for the individual electrode pairs in Fig. 4, in which values measured previously are also included and in which the maximum current is plotted. Above a certain surface area the current amplitude in the range of surface areas considered here does not vary any more.

With small electrodes there is only a small dependence of the maximum current amplitude on the initial pressure although the conductivity of the plasma varies with initial pressure by a factor of two, cf. [4]. With large electrodes this dependence is more pronounced, as shown by previous measurements [4].

Fig. 5 shows this dependence for one pair of electrodes. The values measured previously are also plotted (dashed curve) for comparison (the magnetic field in the first case is a little higher, but the external resistance is also higher, and so comparison is justified, cf. [4]).

This small pressure dependence of the current is also present when 25 electrode pairs are used.

One large electrode pair, 3×7 cm^2 *surface area*

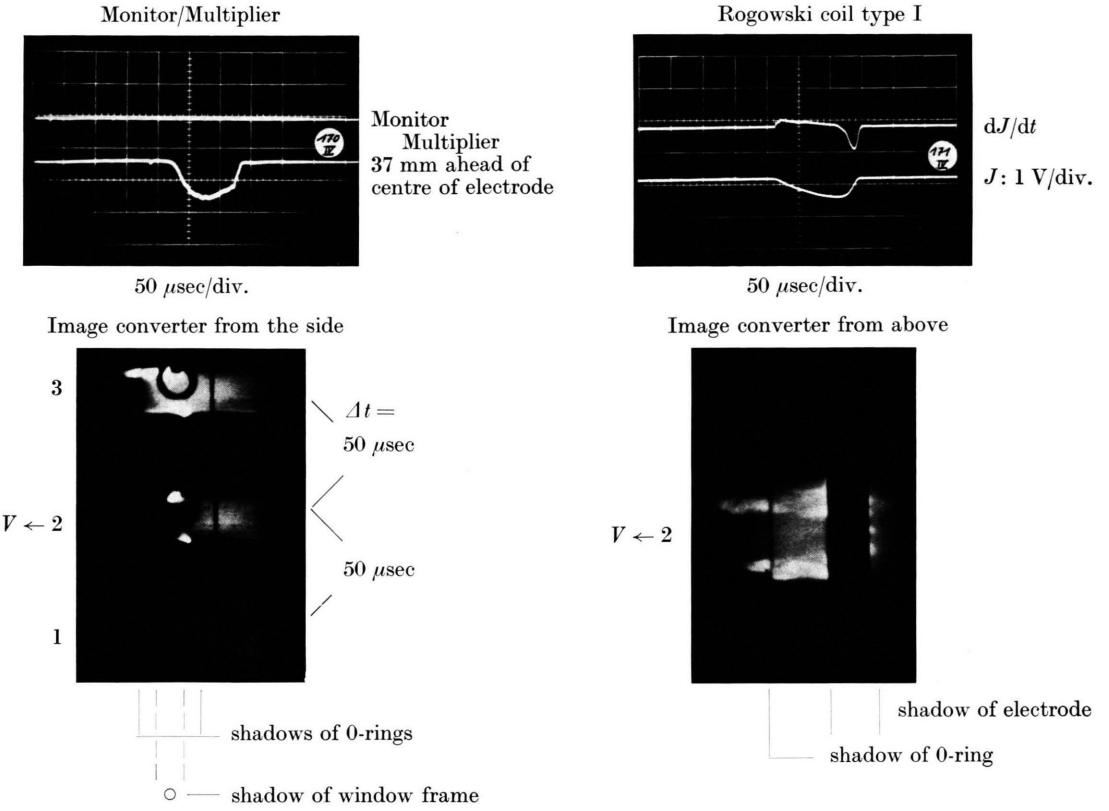

One small electrode pair, 4.5 mm *in diam. in the centre of the measuring chamber*

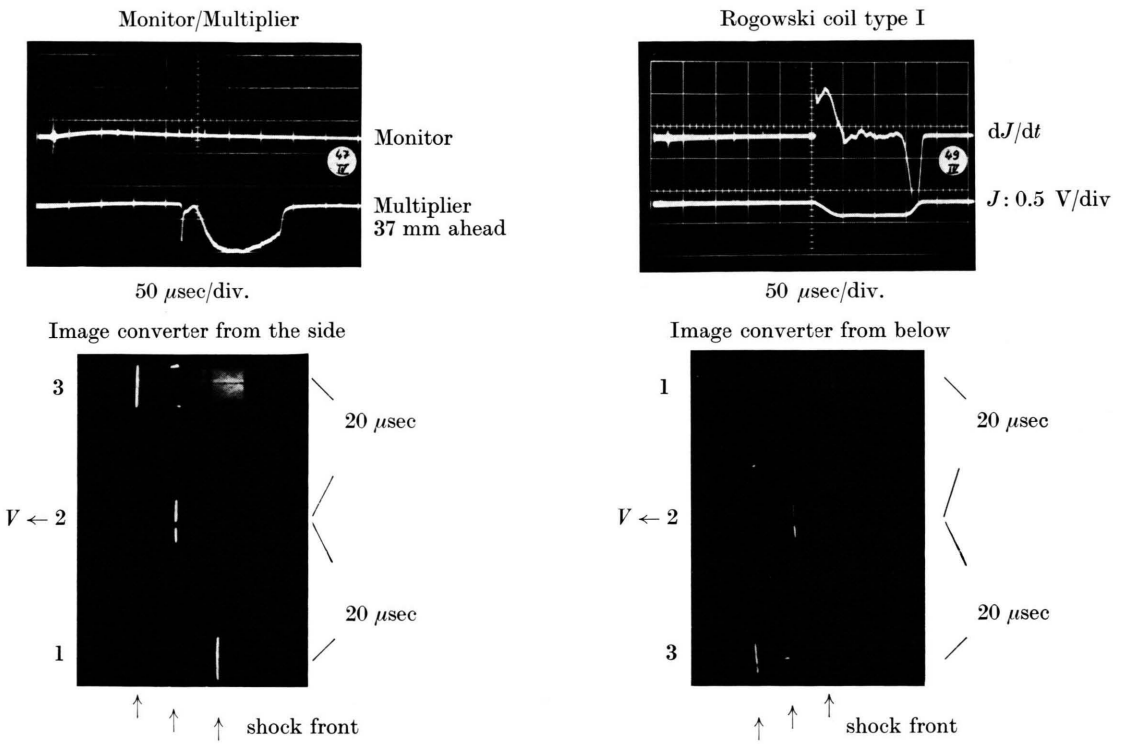

Fig. 1a. Oscillograms and image converter pictures $B_0 = 6.8$ kG, $p_0 = 1$ torr.

Five small electrode pairs transverse to the flow

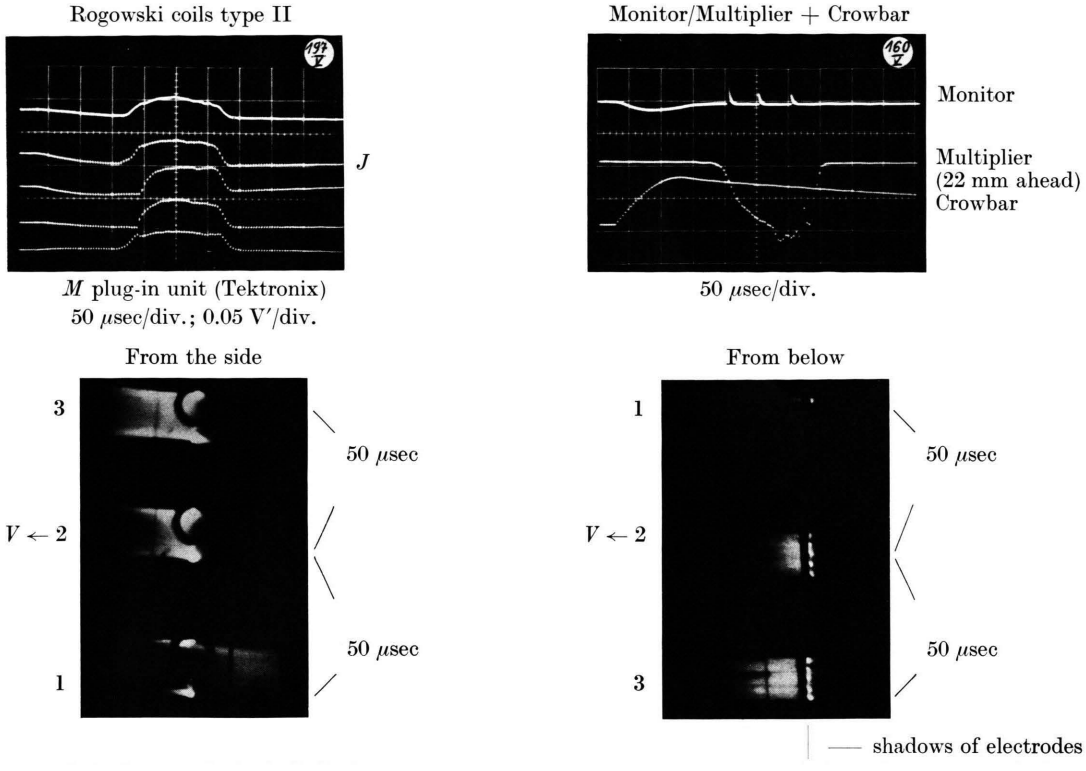

25 small electrode pairs

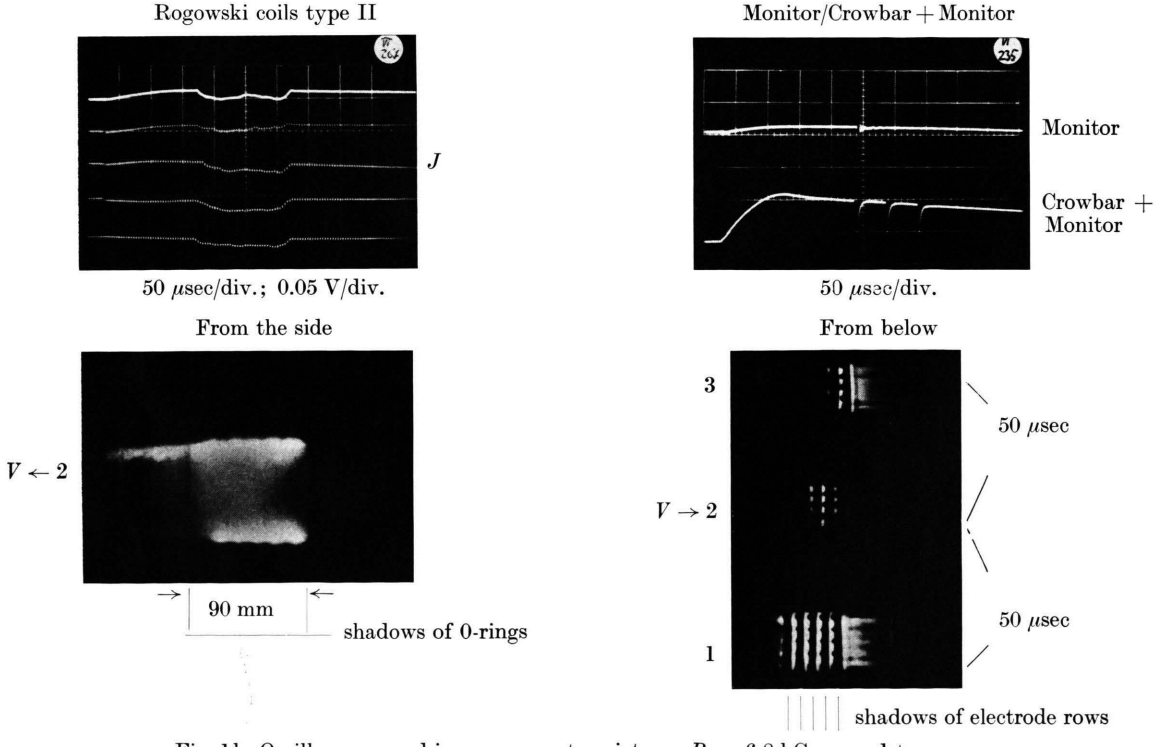

Fig. 1b. Oscillograms and image converter pictures $B_0 = 6.8$ kG, $p_0 = 1$ torr.

V Bd voltage

One electrode pair in the centre of the measuring chamber

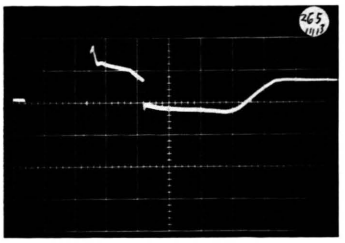

with noise signal from crowbar

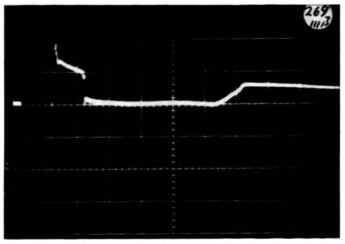

↑ shock front

$p_0 = 1$ torr; 120 V/div.; 50 μsec/div.

↑ shock front

$p_0 = 10$ torr; 120 V/div.; 100 μsec/div.

Multiplier oscillograms behind interaction region

Multiplier + Time marker

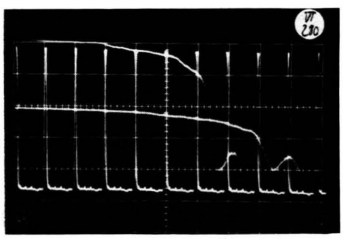

Centre-to-centre distance between multipliers 25,5 mm

↑ ↑

Primary shock front

$p_0 = 1$ torr; 5 μsec/div.

Secondary fronts

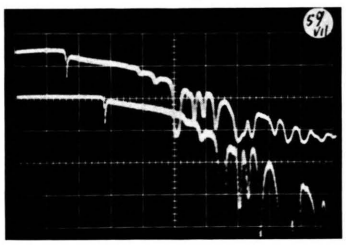

$p_0 = 5$ torr; 20 μsec/div.

Fig. 1 c. Oscillograms, $B_0 = 6.8$ kG.

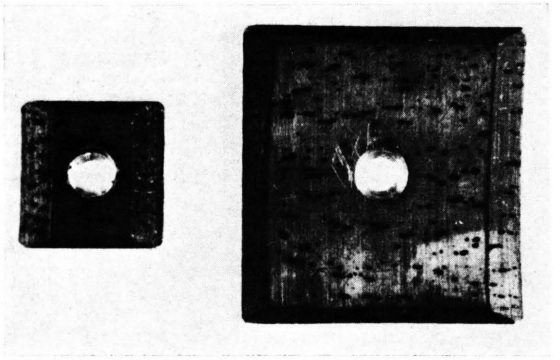

a) Copper anodes of different areas after many shots.

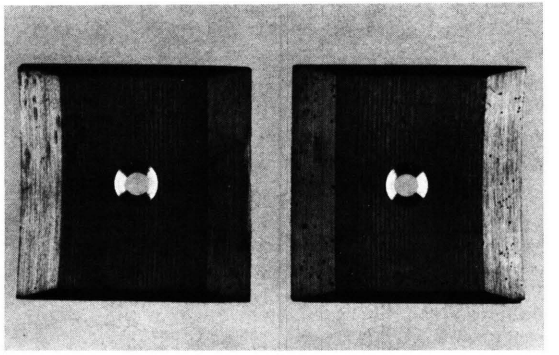

Cathode Anode

b) (made of brass) after one shot, 5×5 cm^2.

$V \leftarrow$

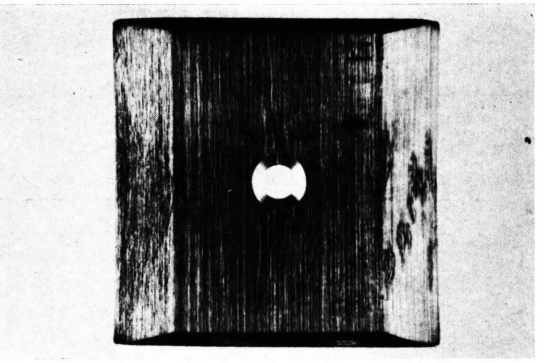

d) Brass cathode, 5×5 cm^2. After *one* shot Chemically and mechanically cleaned beforehand. No spots were observed on the corresponding, likewise cleaned anode.

$V \rightarrow$

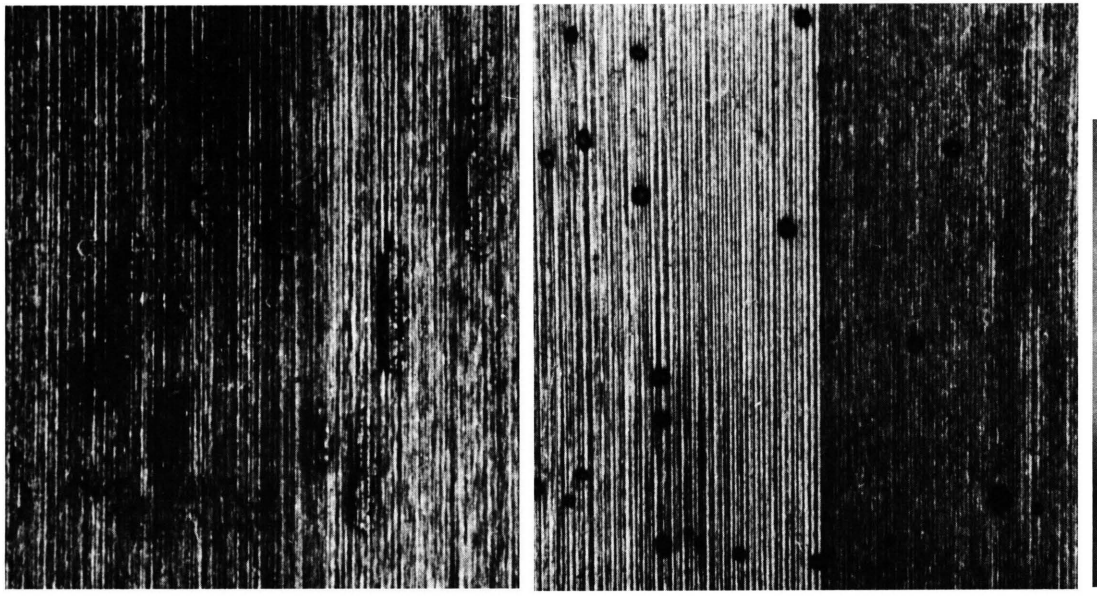

c) Enlarged sections of b) (see Fig. 27 in [4]).

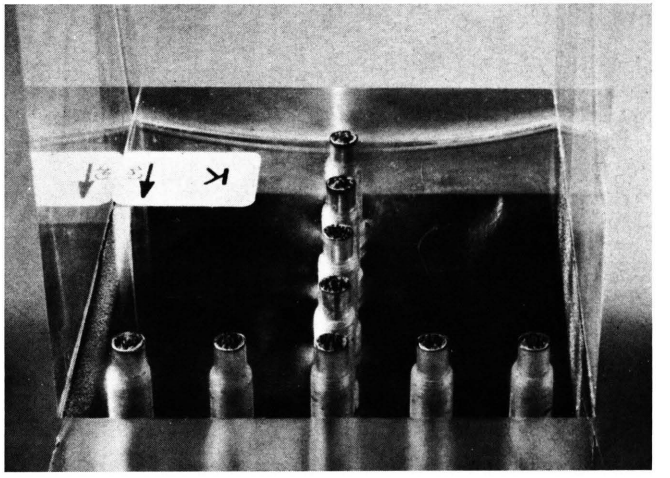

e) Brass cathodes of small area, 4.5 mm in diam. After many shots.

Fig. 6. Spots on anodes and cathodes, cf. [4].

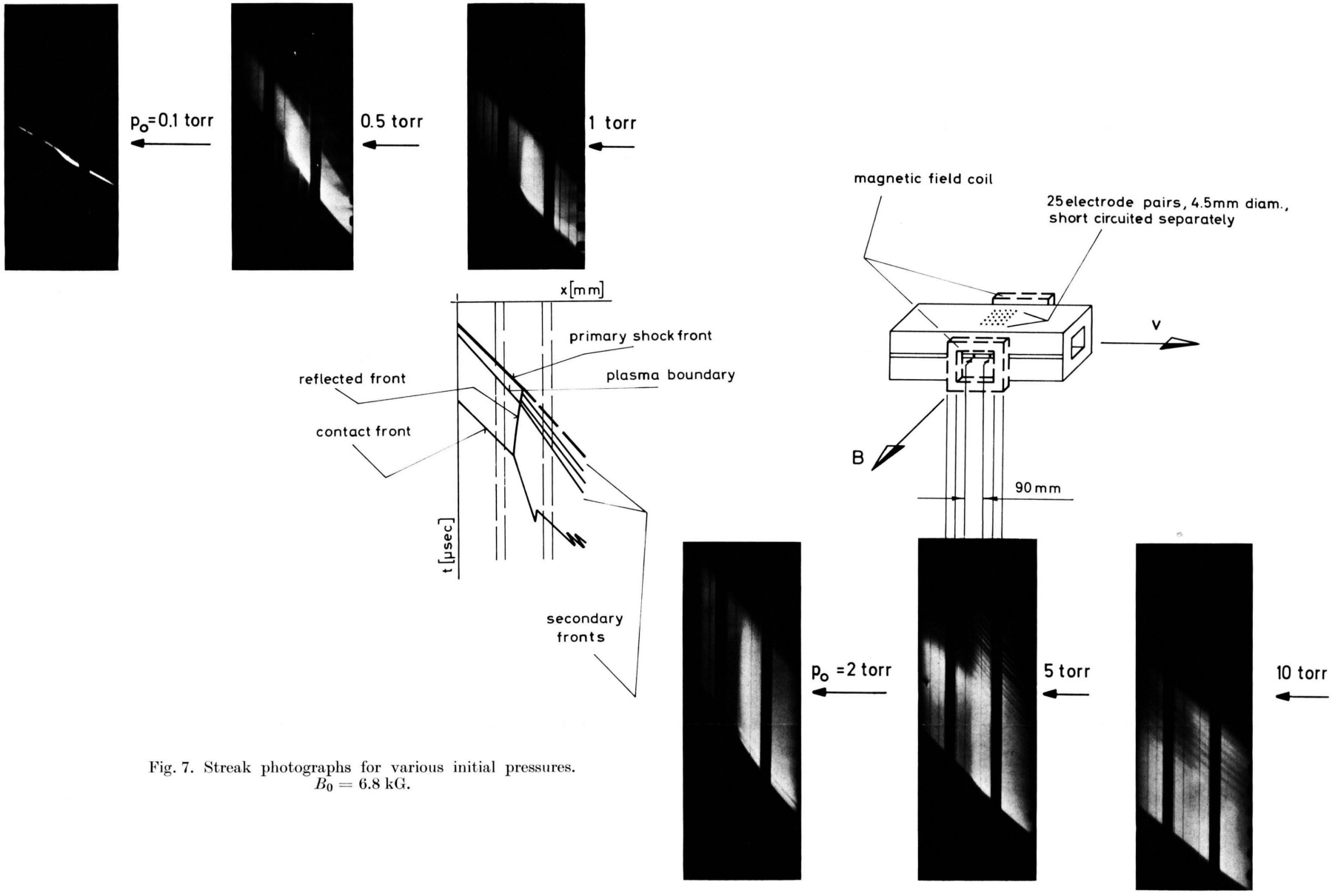

Fig. 7. Streak photographs for various initial pressures. $B_0 = 6.8$ kG.

Fig. 8. Streak picture. $p_0 = 0.5$ torr, $B_0 = 6.8$ kG.

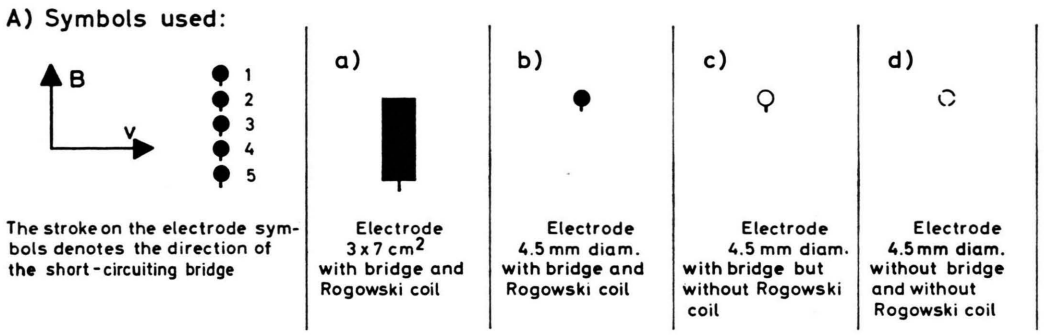

bridge no.			1 bridge and coil shifted in succession from electrode to electrode 5		I II III IV V	I II III IV V	I II III IV V
1			0.7	0.45			0.44
2			0.8	0.65			0.50
3	3.5	0.9	0.9	0.60	0.5 0.5 0.5 0.4 0.7	0.45 0.45 0.40 0.35 0.40	0.51
4			0.8	0.50			0.60
5			0.7	0.45			0.52
Σ	3.5	0.9	3.9	2.7	2.6	2.1	2.6
per pair on the average	3.5	0.9	0.8	0.55	0.54	0.42	0.52

bridge no.	I II III IV V	I II III IV V	I II III IV V coils shifted in succession from row to row I II III IV V	Σ	I II III IV V
1	0.39	0.34	0.24 0.25 0.23 0.20 0.37	1.29	0.19
2	0.38	0.41	0.30 0.30 0.29 0.23 0.33	1.45	0.29
3	0.35	0.30	0.34 0.28 0.20 0.19 0.27	1.28	0.24
4	0.39	0.46	0.31 0.17 0.26 0.15 0.24	1.13	0.16
5	0.44	0.39	0.24 0.21 0.24 0.17 0.28	1.14	0.21
Σ		1.90	1.43 1.21 1.22 0.94 1.49	6.29	1.09
per pair on the average	0.39	0.38	0.25		

Table 1. Results of current measurements for various electrode configurations. Arithmetic mean values of integral mean values with respect to time of the *current in kA*, $p_0 = 1$ torr, $B_0 = 6.8$ kG.

4. Arc spots

The existence of arc spots on large electrodes has already been pointed out in previous investigations [4], but it has not been the subject of any detailed discussion. Such spots were also observed in the investigations described here. Fig. 6 shows pictures of spots that appeared on the cathodes and anodes. On the anodes there appear small round spots that are spread over the entire surface (Fig. 6a, b, c). The spots on the cathodes (Fig. 6b, c) are irregular in shape. The arc spots move along and also across the grooves caused by machining. If the surface is chemically and mechanically cleaned, there are

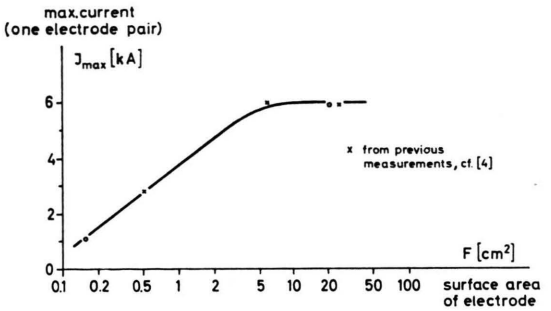

Fig. 4. Max. current vs. surface area of electrode (one electrode pair).

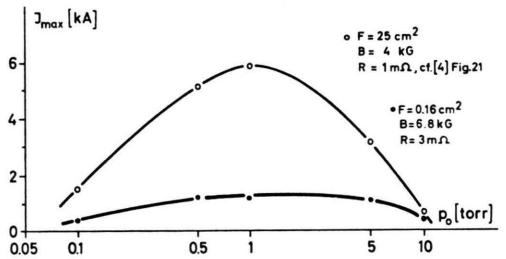

Fig. 5. Max. current vs. initial pressure for one pair of electrodes of large (see [4]) and small area.

then no arc spots on the anodes and those on the cathodes change shape (Fig. 6d). Many traces that look like Lichtenberg figures can be seen branching out in the flow direction (right-hand side).

The round spots on the anodes are thus due to thin layers of impurities. This phenomenon has also been observed in ordinary arcs without magnetic field and transverse flow[5]. The branching observed on "clean" cathodes is in the flow direction of the plasma. It is very improbable that spots move along different branches so as to converge to one point. Much more probable is a development of the spot into many branches. The spots thus presumably move opposite to the $j \times B$ forces. This may be a kind of retrograde motion typical of arcs in magnetic fields. The spots on the small electrodes are also quite distinct (Fig. 6c).

The spots, which are proof of the existence of arcs, thus exhibit all the features known from arc physics.

5. *Internal resistance*

A mean value of the internal resistance can be estimated for the centre of the current pulse, for which dJ/dt can be neglected. With one electrode pair it is possible to use a simple equivalent circuit diagram, cf. [4]. When five electrode pairs transverse to the flow direction are used (in which case the shock front reaches all electrodes at the same time and the voltage E is therefore produced at the same time), it begins to become more difficult to design an equivalent circuit diagram because of, for instance, the inductive coupling of the circuits. When 25 pairs are used, the procedure becomes more difficult in that the shock front reaches the rows of electrodes at different times, and hence the voltage E is applied at various times. At $p_0 = 1$ torr, for instance, this time difference between the first and the fifth rows is 15 μsec. In the latter cases the term $L(dJ/dt)$ cannot be neglected, even in the centre of the current pulse, because this term is multiplied by the number of circuits coupled. For an approximate estimate only the inductive coupling is considered, and one gets the following values shown in Table 2 for $p_0 = 1$ torr. (Here the influence of the magnetic field of the current and the influence of a decrease of the velocity was not taken into account.)

1 pair		5 pairs	25 pairs
large electrodes	small electrodes	small electrodes	small electrodes
25 mΩ	140 mΩ	190 mΩ	400 mΩ

Table 2. Internal resistance per circuit for $p_0 = 1$ torr.

The change of this value of the internal resistance merely reflects the variation of the current with, for example, the number of electrode pairs. The external resistance of 3 mΩ is small compared to these values.

6. *Calculation of the retarding $j \times B_0$ force*

The real aim here is to fill the interaction volume with current as uniformly as possible. The image converter pictures suggest that this has been achieved using 25 electrode pairs. There is, however, a certain amount of bulging in the flow direction. The current density distribution is not known, of course, but it seems reasonable to assume that it is uniform in the electrode region. On this assumption, it is possible to calculate roughly the retarding force acting on the plasma. (Here only the external magnetic field B_0 is taken into account. In approximation, the B_z field is reduced by the currents at the beginning of the interaction region and in-

[5] J. M. SOMERVILLE, and C. T. GRAINGER,, Brit. J. Appl. Phys. 7, 109 [1956].

creased at the end. The mean field is again B_0. On the other hand, the magnetic Reynolds number is small, cf. Table III.)

The total hydrodynamic pressure of the unperturbed flow

$$p_1 + \varrho_1 v_1^2$$

can also be calculated, cf.[4].

Table 3 shows the calculated ratio of the retarding force per unit area to the total hydrodynamic pressure for various initial pressures. L is the interaction length. The table also includes the calculated magnetic Reynolds numbers.

p_0 torr	$\frac{j B_0 L}{p_1 + \varrho_1 v_1^2}$	$R_m = \frac{\mu_0 j L}{B_0}$
0.5	0.7	0.18
1	0.5	0.18
2	0.3	0.18
5	0.2	0.18
10	0.04	0.07

Table 3. Ratio of retarding force per unit area to the total hydrodynamic pressure of the flow for various initial pressures, and magnetic Reynolds numbers. 25 electrode pairs. $B_0 = 6.8$ kG.

The retarding force should have a noticeable effect of slowing down the plasma, at least at low initial pressures, because the retarding force is of the order of the total hydrodynamic pressure.

7. Results of drum camera measurements

Fig. 7 shows some streak pictures taken over the entire length of the measuring chamber with p_0 as parameter. B_0 is 6.8 kG. Number of electrodes is 25. At $p_0 = 0.1$ torr, the plasma slab is not long enough to allow interaction effects to be clearly recognized. It can be seen, however, that the plasma is deflected in the interaction region.

At $p_0 = 0.5$ torr, the plasma flow makes a sharp bend in the interaction region thus indicating a decrease of velocity. There is another front which runs counter to the flow until it reaches the contact front and is reflected from it in the downstream direction, finally catching up with the primary front. These fronts can be recognized more clearly in the colour photograph in Fig. 8.

At $p_0 = 1$ torr, the reflected front becomes more obvious, the bend in the flow less so. Secondary fronts can be observed behind the primary front. (These were also detected with multipliers, see Fig. 1).

With increasing pressures above $p_0 = 2$ torr, the velocity of the reflected front decreases until it comes to rest in the flow and is finally carried along by it. The number of secondary fronts increases with the initial pressure (see again Fig. 1). All streak pictures show the velocities of the reflected fronts to be time dependent.

A device for differentiating curves was used to evaluate the streak pictures with respect to the velocity of the reflected fronts. The results are shown in Fig. 9. The direction of the flow velocity v_1 behind the primary shock front is taken as positive. The relative values refer to the calculated flow velocity v_1, which the plasma has behind the unperturbed primary shock front. The arrows indicate the development with time. At low initial pressures p_0, the reflected fronts decrease to the flow velocity v_1. At high initial pressures, the front is swept along by the flow (reversal of direction). Fig. 10 shows the velocity of that front which is again reflected at the contact front for $p_0 = 0.5$ torr. This front leaves the interaction region and its velocity increases in the downstream direction.

Behind the primary front one can observe secondary fronts, which are the stronger the higher the initial pressure p_0. The velocity of the first secondary front at $p_0 = 1$ torr is, for example, 2.7 ± 0.1 mm/μsec.

8. Results of photomultiplier measurements

The multiplier measurements yield the velocities U_s or the shock Mach numbers M_s of the primary shock in front of and behind the interaction region. In addition, the velocity U of the first secondary front behind the primary shock front was determined after it has passed through the interaction region. The secondary fronts were observed with the multipliers from two directions that are mutually perpendicular and perpendicular to the shock tube axis. The shock Mach numbers can be used to calculate the parameters of the gas behind the shock front. Table 4 shows the results for $p_0 = 1$ torr.

III. Discussion

The total internal resistance is composed of the internal resistance of the current channel in the plasma flow and that of the plasma-to-electrode transition. The conductivity of the plasma is very high. Therefore, the high internal resistance

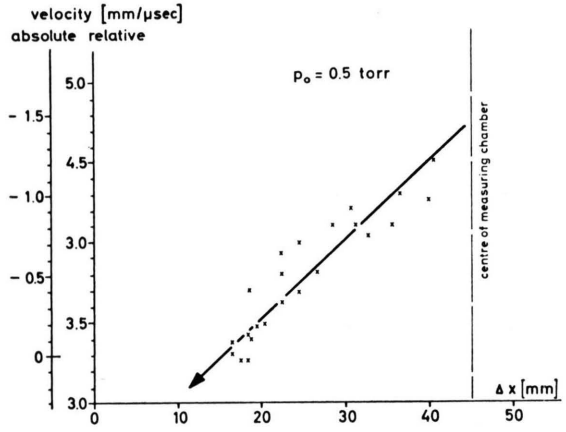

9 a

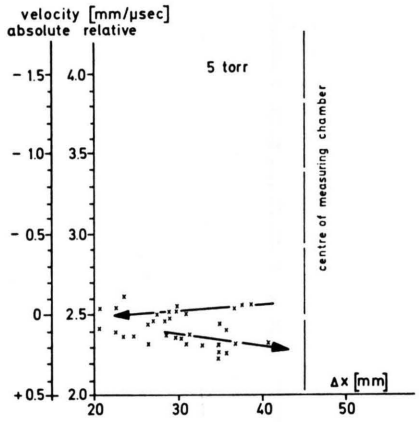

9 b

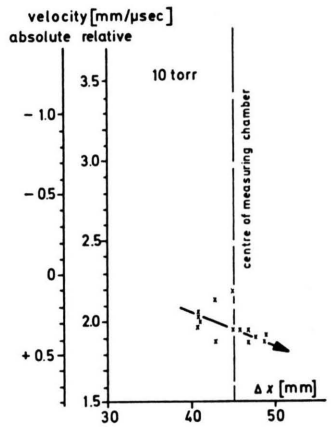

9 c

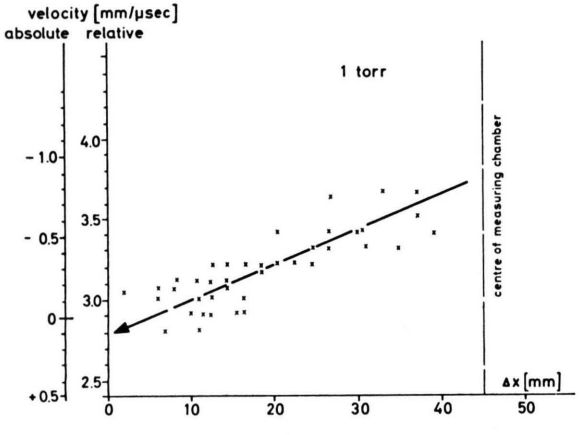

9 a

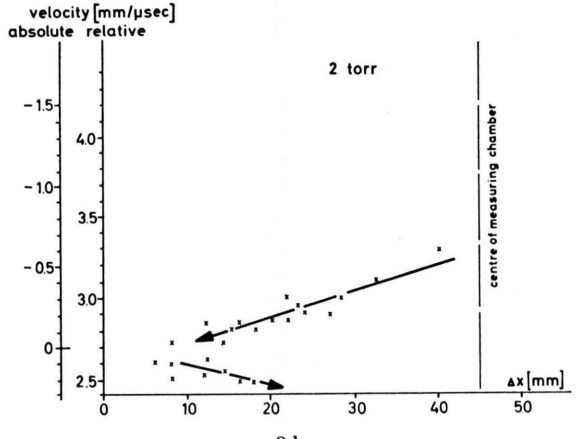

9 b

Fig. 9a. Velocities of reflected fronts. The relative values refer to the flow velocity. The arrows indicate the development with time.
Fig. 9b. See Fig. 9a.
Fig. 9c. See Fig. 9a.

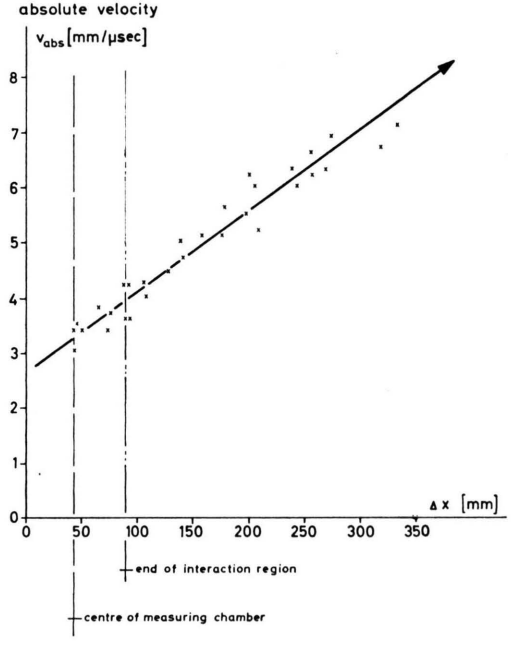

Fig. 10. Velocity of front reflected at contact front for $p_0 = 0.5$ torr.

In front of interaction region			Behind interaction region in downstream direction			
Shock front velocity	Shock Mach number	Flow velocity	Shock front velocity	Shock Mach number	Flow velocity	Velocity of secondary front
U_s [mm/μsec]	M_s	v_1 [mm/μsec]	U_s [mm/μsec]	M_s	v_1 [mm/μsec]	U [mm/μsec]
3.6 ± 0.1	11.5 ± 0.3	2.9 ± 0.1	3.1 ± 0.1	10 ± 0.3	2.4 ± 0.1	2.7 ± 0.1

Table 4. Results of multiplier measurements.

occurring for small electrodes can only be formed by the plasma-to-electrode transition and not by the plasma itself. This transition is formed by the arc channels leading to the arc spots and by the arc spots themselves. The spots exhibit all the features described in the literature on normal arcs, e.g.[6]. It therefore seems reasonable to compare the phenomena here with those of normal arcs. The pictures of the arc spots demonstrate that the arcs are of the type with non-stationary spots. In such arcs small spots appear and disappear continually on the cathode. The narrow current channels to the arc spots are of high density, viz. up to 10^6 A/cm^2. Despite numerous investigations, the transition phenomena in normal arcs have not yet been explained quantitatively because the conditions in the transition are extremely complex. These conditions, however, govern the current amplitude and density.

Since our case is even more complicated, the difficulties confronting quantitative interpretation of the results of current measurements can only be overcome, if at all, by numerous investigations of the boundary phenomena. This, however, would go beyond the scope of this experiment. No predictions can therefore be made, and so the currents have to be measured again for every change of the geometry or of a parameter. It is not known, for example, whether the current becomes larger or even smaller with higher magnetic field. The current density cannot be calculated, as is done, for example, in MHD generators. The results of the current measurements can only be understood qualitatively:

a) In order to check the dependence of the current on the electrode surface area below a certain size, let us study the pictures of the arc spots (Fig. 6). In the case of large electrodes there are many arc spots, at some distance from one another. The current amplitude must be governed by the number of spots. On the other hand, a certain distance is expected between the spots, i.e. between the current channels, owing to the space charge density distribution in front of the cathode. In the case of small electrodes there is no such minimum distance, and the number of arc spots, and hence the current amplitude, should become smaller.

b) The decrease of the current amplitude with the number of electrode pairs can be explained by the mutual influence of the space charges in front of the electrodes. This affects the formation of spots, the number of which governs the current amplitude.

c) The small influence of the initial pressure p_0, i.e. of the conductivity of the streaming plasma, on the current amplitude in the case of small electrodes is due to the fact that the current amplitude is governed essentially by the plasma-to-electrode transition, not by the plasma itself. In the case of large electrodes, the arc spots together provide so much current that the internal resistance of the transition becomes comparable with that of the streaming plasma.

d) The time variation of the current (dJ/dt) in the centre of the current pulse is smallest for one pair of large electrodes and largest for 25 pairs of small electrodes. This is because there are so many arc spots on large surfaces that the effect of their migration, disappearance, and appearance is averaged out in time, approximately at least. In the case of small surfaces, however, the effect may become more pronounced especially when 25 electrode pairs are involved, because the potential distribution is of a very complicated nature owing to the mutual influence of the current channels. (Moreover, the slowing down of the plasma flow may have an effect in the latter cases.)

The total current that can be drawn using many small electrodes is not much higher than that for large electrodes, but the current distribution is

[6] W. Finkelnburg, and H. Maecker,, Handbuch der Physik, Vol. XXII.

certainly much more uniform. When 25 electrode pairs are used, the retarding force jBL is of the order of the total hydrodynamic pressure of the flow. Using more small electrodes in the flow direction will elongate the interaction length L, but on the other hand the total current will decrease, see Fig. 3. Extrapolating from Fig. 3 one can estimate that using more electrodes will not produce an appreciably stronger retarding force. Using fewer electrodes, for instance five pairs, transverse to the flow direction will produce a smaller retarding force. Another possibility is the use of a smaller number of electrodes with larger surface area. This would influence the current distribution. Choosing 25 pairs of electrodes therefore seems to be a reasonable compromise.

As expected from the estimate of the retarding forces, cf. Table 3, the plasma flow is slowed down. The velocity of the reflected fronts decreases with increasing initial pressure. This agrees with the calculated decrease of the retarding force with growing initial pressure. The local velocity of sound in the unperturbed plasma is 1.6 mm/μsec. The reflected fronts observed therefore travel with supersonic velocity relative to the streaming plasma. Their Mach number varies between 2.8 and 1.3 depending on the initial pressure.These are probably shock waves. This is supported by the fact (which can be clearly recognized in the case of $p_0 = 0.5$ torr) that reflection takes place again at the contact front. Values of shock Mach numbers between 2.8 and 1 are quite possible theoretically. There is, however, reason for concluding that relaxation effects are involved and so, strictly speaking, the observed luminous fronts are not the shock fronts. One reason is that the "sharpness" of the fronts diminishes with decreasing initial pressure. This would explain why such fronts could not be recognized in the image converter photographs and in the multiplier oscillograms.

The velocity of the primary shock front is reduced after it has passed through the interaction region, as the results of, for example, the multiplier measurements at $p_0 = 1$ torr show. But the flow velocity behind this shock front is still supersonic, see Table 4. On the other hand, the flow velocity behind the reflected shock must be subsonic. This indicates the existence of a fan of rarefaction waves which, according to the theory[1/2], accelerate the plasma from the subsonic velocity behind the reflected shock to the supersonic velocity behind the primary shock.

The increasing velocity of the twice reflected front at, for instance, $p_0 = 0.5$ torr, even after it has left the interaction region (Fig. 10), can be explained by the mutual influence of this front and the fan of rarefaction waves. According to the theory[7] an interaction between a shock front and a fan of rarefaction waves will accelerate the shock front.

The secondary fronts observed behind the primary shock front in the streak pictures and multiplier oscillograms can also be detected, especially at higher initial pressures in measurements without magnetic field, i.e. without any external influence on the plasma flow[8]. These fronts are produced when very small particles of impurities (dust from the diaphragms) are carried along by the streaming gas. This effect becomes more pronounced here when the gas is heated by the currents. The velocity of these fronts is roughly equivalent to the calculated flow velocity of the plasma behind the primary shock, see Table 4. These particles change the incandescence of the gas. Since this phenomenon can occur in all diaphragm shock tubes, it may distort spectroscopic measurements. But the particles are small enough not to disturb the flow, which is proved by interferometric measurements (see, for example, Fig. 8 in[9]). The advantage in our case is that it is thereby possible to determine approximately the flow velocity, this being very difficult otherwise.

IV. Concluding Remarks

The result of these investigations suggest that it is possible to utilize the arcs produced by $\boldsymbol{v} \times \boldsymbol{B}$ forces to achieve an approximately uniform current distribution such that the gasdynamic effects resulting from $\boldsymbol{j} \times \boldsymbol{B}$ interaction can be described by a theory which, though transient, is one-dimensional.

Other investigations, mainly quantitative, will be necessary, however, to obtain confirmation. Mach-Zehnder interferometer measurements, for instance,

[7] A. G. Bird, J. Fluid. Mech. **15**, 282 [1963].
[8] H. Nett, Report IPP 3/43, October [1966].
[9] H. Klingenberg and A. Siddiqui, Z. Naturforschg. **23a**, 752 [1968].

were begun to prove that the observed fronts are plane shock fronts and to detect other gasdynamic effects. In addition, the electron and neutral atom densities behind the fronts are to be measured. Only then can the experimental results be reasonably compared with the theory.

The transient part of the theory of JOHNSON[2] describing effects in the interaction region can be taken as a basis. However, the assumption made in this theory that the current density can be expressed in terms of $\sigma v B$ is not valid. The current density has to be determined experimentally. Furthermore, ionization effects have to be taken into account.

A theory describing the flow pattern after reflection of the reflected front at the contact front has yet to be formulated.

In further experiments it is hoped to produce reflected shocks leaving the interaction region by increasing the magnetic field, i.e. the retarding force. If then a sort of steady state can be achieved, the theory of REBHAN[1] can be taken as a basis, allowance again being made for ionization effects.

The author wishes to thank Prof. WIENECKE and Dr. MUNTENBRUCH for encouragment and useful discussions. He is indebted to Mr. SCHMID, STEFFES and LOEBEL for technical assistance.

This work has been undertaken as part of the joint research programme of the Institut für Plasmaphysik and Euratom.